On wind turbine down-regulation control strategies and rotor speed set-point

Lio, Wai Hou; Mirzaei, Mahmood; Larsen, Gunner Chr.

Published in:
Journal of Physics: Conference Series

Link to article, DOI:
10.1088/1742-6596/1037/3/032040

Publication date:
2018

Document Version
Publisher's PDF, also known as Version of record

On wind turbine down-regulation control strategies and rotor speed set-point

IOP Conf. Series: Journal of Physics: Conf. Series **1037** (2018) 032040 doi:10.1088/1742-6596/1037/3/032040

On wind turbine down-regulation control strategies and rotor speed set-point

Wai Hou Lio, Mahmood Mirzaei and Gunner Chr. Larsen

Department of Wind Energy, Technical University of Denmark, DK-4000 Roskilde, Denmark

E-mail: wali@dtu.dk

Abstract.

The use of down-regulation or curtailment control strategies for wind turbines offers means of supporting the stability of the power grid and also improving the efficiency of a wind farm. Typically, wind turbine derating is performed by modifying the power set-point and subsequently, the turbine control input, namely generator torque and blade pitch, are acted on to such changes in the power reference. Nonetheless, in addition to changes in the power reference, derating can be also performed by modifying the rotor speed set-point. Thus, in this work, we investigate the performance of derating strategies with different rotor speed set-point, and in particular, their effect on the turbine structural fatigue and thrust coefficient were evaluated. The numerical results obtained from the high-fidelity turbine simulations showed that compared to the typical derating strategy, the derated turbines might perform better with lower rotor speed set-point but it is crucial to ensure such a set-point does not drive the turbine into stalled operations.

1. Introduction

Large wind turbines in a wind farm are often curtailed or down-regulated for the purposes of stabilising the power grid [1] or improving the efficiency of wind farms [2]. For example, the power references for turbines is set to comply with the orders of the power grid operators (e.g. [3]) or down-regulation of the upstream turbines could improve the power production of the entire wind farm (e.g. [2, 4, 5]). Typically, in nominal operations, the control objective of a wind turbine is to maixmise its power production in the below-rated wind conditions and operate at the rated power in the above-rated wind conditions. The control inputs (pitch angles and generator torque) and rotor speed set-point are pre-defined that leaves limited rooms to manoeuvre. In contrast, in derated operations, wind turbines operate at a lower efficiency compared to nominal operations, thus, it allows the turbine controller to interpret the power set-point, with more freedoms, into different sets of control inputs and rotor speed set-point. Consequently, this motivates the development of derating control strategies that not only can track the power set-point, but also take into account other factors such as the fatigue of key turbine components and the generated downstream wake.

In the past, studies were mainly focused on improving the controller performance in nominal operations (e.g. [6, 7]), whilst derating was simply performed by keeping the rotor speed at the rated value and adjusting the generator torque set-point (e.g. [8, 9]). In recent years, a growing body of research has emerged, seeking to improve the controller design for derating operations. An earlier study [10] proposed the usage of the rotor speed set-point for the turbine

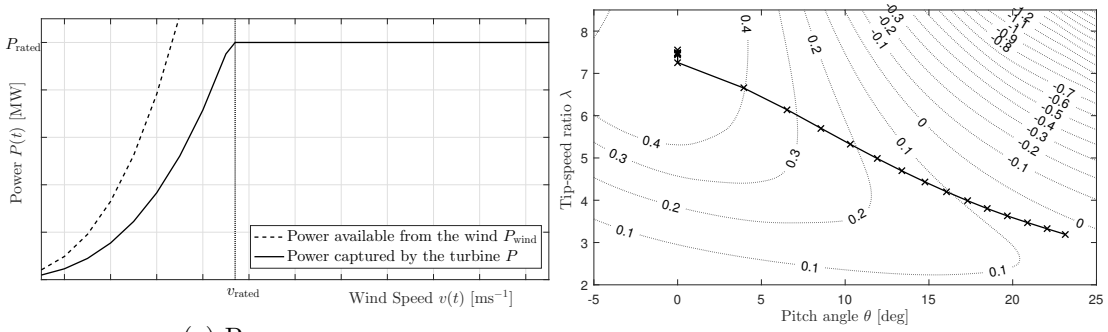

(a) Power curve.

(b) Power coefficient C_{p}.

Figure 1: Power curves and operating points of a NREL 5MW turbine [17].

controllers to improve the transient performance and stalling during derating operations. Later, the authors in [11] developed a derating strategy that relieves the burden on the blade pitch during derating operations, that is achieved by updating the rotor speed set-point on-line based on the power output and the torque controller acted upon the rotor speed set-point. In [12], the authors investigated three derating control strategies operating based on different rotor speed set-points, and the performance of these three derating methods in a wind farm was examined by [13, 14]. The studies (e.g. [15] and [16]) investigated derating strategies that produces the lowest steady-state thrust coefficient for improving the downstream wake effect. .

One key observation from [12, 13] is that derating strategies with different rotor speed set-point would result in different operating points. For example, some studies (e.g. [1]) examined a derating strategy with a maximum (or rated) rotor speed and showed it is beneficial for storing the rotational energy, which allows the turbine to respond to the sudden power demand from the grid. Other studies (e.g. [13, 15, 16]) suggested that turbines operating at a low rotor speed could generate less wake effect downstream. Given that there exists a range of combinations of the power and rotor speed set-points, this begs the question: "what is the optimal rotor speed set-point during derating and with respect to what it is optimal?". Therefore, this work aims to bridge the gap by investigating the relationship between the performance of the derating strategies and rotor speed set-point, and in particular, the fatigue damage on key turbine components and thrust coefficient of each strategy were evaluated.

The remainder of this paper is structured as follows. In Section 2, the background of wind turbine controller is presented. This is followed in Section 3 by the design of derating strategies and the key analysis on their performance with respect to the rotor speed set-point. In Section 4, simulation results on a high-fidelity wind turbine demonstrate the performance of different derating strategies and followed by discussions of the results. Conclusions are in Section 5.

2. Background

This section presents briefly the operations and baseline controller of a typical wind turbine. Figure 1a depicts the power curves of the power available from the wind and the power captured by a typical wind turbine. The power available $P_{\text{wind}}(t)$ for a typical wind turbine is a function of the cube of the free-stream wind speed $v(t)$, defined as follows:

$$P_{\text{wind}}(t) := \frac{1}{2}\rho\pi r^2 v^3(t), \tag{1}$$

where $\rho, r \in \mathbb{R}$ are the air density and blade length. The power available from the wind $P_{\text{wind}}(t)$ cannot be fully captured by a turbine and the captured power $P(t)$ depends on the aerodynamic

efficiency (or power coefficient) $C_{\mathrm{p}} : \mathbb{R} \times \mathbb{R} \to \mathbb{R}$ of the turbine, defined as follows:

$$P(t) := \frac{1}{2}\rho\pi r^2 v^3(t) C_{\mathrm{p}}(\lambda, \theta)\eta, \tag{2}$$

where the free-stream wind speed $v(t) \in [v_{\mathrm{in}}, v_{\mathrm{out}}]$ is within the cut-in and cut-out wind speed and $\eta \in \mathbb{R}$ denotes the efficiency of the generator converter. The tip-speed ratio $\lambda(t)$ is defined as follows:

$$\lambda(t) = \frac{\omega(t) r}{v(t)}, \tag{3}$$

where $\omega(t)$ denotes the rotor speed and its dynamics can be described as follows:

$$J_{\mathrm{r}}\dot{\omega}(t) = \tau_{\mathrm{a}}(\lambda, \theta) - \tau_{\mathrm{g}}(t), \tag{4}$$

where $J_{\mathrm{r}} \in \mathbb{R}$ denotes the moment of inertia of the rotor, whilst the aerodynamic and generator torque on the rotor are $\tau_{\mathrm{a}} : \mathbb{R} \times \mathbb{R} \to \mathbb{R}$ and $\tau_{\mathrm{g}}(t)$. The control inputs to a typical wind turbine are the pitch angles $\theta(t)$ and generator torque $\tau_{\mathrm{g}}(t)$.

As depicted in Figure 1a, a variable-speed wind turbine typically operates based on two operating wind conditions. In the below-rated wind conditions where the wind speed $v(t)$ is lower than the rated wind speed $v_{\mathrm{rated}} \in \mathbb{R}$, the turbine tends to maximise the power production by operating at maximum aerodynamic efficiency $C_{\mathrm{p_{max}}} \in \mathbb{R}$, whilst in the above-rated wind conditions where the wind sped $v(t)$ is higher than the rated wind speed v_{rated}, the turbine operates at the rated power $P_{\mathrm{rated}} \in \mathbb{R}$.

Figure 1b shows a power coefficient $C_{\mathrm{p}}(\lambda, \theta)$ curve of a typical turbine. In order to achieve maximum power coefficient $C_{\mathrm{p_{max}}}$ in the below-rated wind conditions, the pitch angle $\theta(t)$ is set around 0 degrees and the tip-speed ratio $\lambda(t)$ is at the optimal tip-speed ratio $\lambda_{\mathrm{opt}} \in \mathbb{R}$. Thus, given the optimal tip-speed ratio, the optimal rotor speed set-point $\omega_{\mathrm{sp}}(t)$ at given wind speed can be calculated based on (3). Typically, the generator torque is employed to track the rotor speed set-point using, for example, a proportional-integral-derivative (PID) control design. Note that the rotor speed set-point reaches the rated rotor speed $\omega_{\mathrm{rated}} \in \mathbb{R}$ at wind speed $v_\omega \in \mathbb{R}$, which is typically lower the rated wind speed v_{rated}. In contrast, in the above-rated wind conditions, the power output is maintained by regulating the rotor speed at rated using the pitch angle $\theta(t)$ and the generator torque is kept at rated $\tau_{\mathrm{rated}} := \frac{P_{\mathrm{rated}}}{\omega_{\mathrm{rated}}} \in \mathbb{R}$.

Therefore, typical wind turbine controllers are as follows (e.g. [18]):

$$\omega_{\mathrm{sp}}(t) = \begin{cases} \frac{\lambda_{\mathrm{opt}} v(t)}{r}, & v < v_\omega, \\ \omega_{\mathrm{rated}}, & v \geq v_\omega, \end{cases} \tag{5a}$$

$$\tau_{\mathrm{g}}(t) = \begin{cases} K_{\mathrm{P}}^{\tau_{\mathrm{g}}}(\omega(t) - \omega_{\mathrm{sp}}(t)) + K_{\mathrm{I}}^{\tau_{\mathrm{g}}}(\omega(t) - \omega_{\mathrm{sp}}(t)), & v < v_\omega, \\ \tau_{\mathrm{rated}}, & v \geq v_\omega, \end{cases} \tag{5b}$$

$$\theta(t) = \begin{cases} 0, & v < v_{\mathrm{rated}}, \\ K_{\mathrm{P}}^{\theta}(\omega(t) - \omega_{\mathrm{sp}}(t)) + K_{\mathrm{I}}^{\theta}(\omega(t) - \omega_{\mathrm{sp}}(t)), & v \geq v_{\mathrm{rated}}. \end{cases} \tag{5c}$$

Notice that the free-stream wind speed $v(t)$ is the scheduling parameter that determines the operating region the turbine is in. The free-stream wind speed $v(t)$ can be determined by the cup anemometer, wind speed estimator or light detection and ranging (LIDAR) systems.

3. Design and analysis of de-rating strategies

This section presents the control design for derating and followed by the analysis of different derating control strategies and their relationship with the rotor speed set-point.

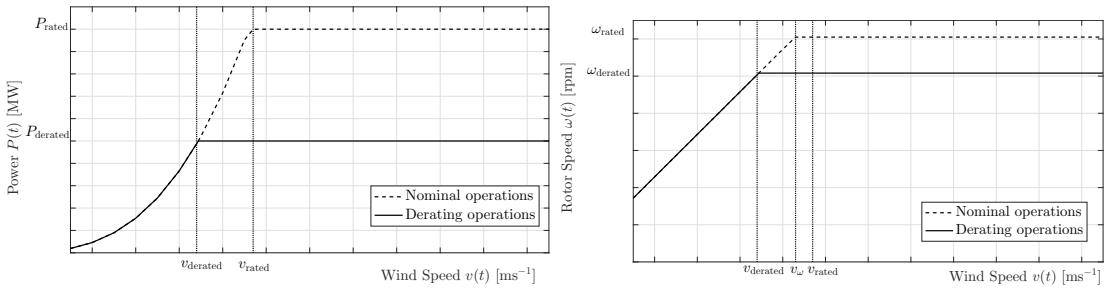

(a) Power curves. (b) Rotor speed operating points.

Figure 2: Nominal and derating operations.

3.1. Design of de-rating control strategies

At first, considering the following definitions:

Definition 3.1 (Derated power)**.** *The derated power* $P_{\text{derated}} \in \{P_{\text{derated}} \in \mathbb{R} | P_{\min} \leq P_{\text{derated}} < P_{\text{rated}}\}$ *is the power output of a turbine demanded to generate in the derating operations, which is typically lower than the rated value* P_{rated} *and above the minimum power output* $P_{\min}$*.*

Definition 3.2 (Derated wind speed)**.** *The derated wind speed* $v_{\text{derated}} \in \{v_{\text{derated}} \in \mathbb{R} | v_{\text{in}} \leq v_{\text{derated}} < v_{\text{rated}}\}$ *is defined as the* ***minimum*** *wind speed needed for the turbine to generate the derated power* P_{derated}*. Thus, the derated wind speed* v_{derated} *can be derived based on* (2) *as follows:*

$$v_{\text{derated}} := \left(\frac{P_{\text{derated}}}{\frac{1}{2}\rho\pi r^2 C_{\text{pmax}}\eta}\right)^{\frac{1}{3}}. \tag{6}$$

Definition 3.3 (Derated rotor speed)**.** *The derated rotor speed* $\omega_{\text{derated}} \in \mathbb{R}$ *is the rotor speed when the turbine reaches the demanded power* P_{derated} *at the derated wind speed* v_{derated}*. The derated rotor speed* ω_{derated} *is derived from* (3) *as follows:*

$$\omega_{\text{derated}} := \frac{v_{\text{derated}}\lambda_{\text{opt}}}{r}. \tag{7}$$

Figure 2a depicts the derating operations compared to the nominal power curve of a typical wind turbine. In derating operations, when the wind speed is not enough to generate the demanded power P_{derated}, i.e. below the derated wind speed v_{derated}, the control objective is the same as the nominal controller to maximise the power production as shown in Figure 2a. However, when the wind speed reaches the derated wind speed v_{derated}, the power is regulated around the derated value P_{derated}. Figure 2b shows the rotor speed in derating operations compared to the nominal case. Notice that when the wind speed is above the derated value v_{derated}, the turbine can choose to operate at any arbitrary rotor speed. Based on Figure 2, the derating features can be incorporating into the turbine baseline controller with two degrees-of-freedom, namely, the set-point of power P_{sp} and rotor speed ω_{sp}, as follows:

$$\omega_{\text{sp}}(t) = \begin{cases} \frac{\lambda_{\text{opt}} v(t)}{r}, & v < v_{\text{derated}}, \\ \omega_{\text{sp}}, & v \geq v_{\text{derated}}, \end{cases} \tag{8a}$$

$$\tau_{\text{g}}(t) = \begin{cases} K_{\text{P}}^{\tau_{\text{g}}}\big(\omega(t) - \omega_{\text{sp}}(t)\big) + K_{\text{I}}^{\tau_{\text{g}}}\big(\omega(t) - \omega_{\text{sp}}(t)\big), & v < v_{\text{derated}}, \\ \frac{P_{\text{sp}}}{\omega_{\text{sp}}}, & v \geq v_{\text{derated}}, \end{cases} \tag{8b}$$

$$\theta(t) = \begin{cases} 0, & v < v_{\text{derated}}, \\ K_{\text{P}}^{\theta}\big(\omega(t) - \omega_{\text{sp}}(t)\big) + K_{\text{I}}^{\theta}\big(\omega(t) - \omega_{\text{sp}}(t)\big), & v \geq v_{\text{derated}}. \end{cases} \tag{8c}$$

Table 1: Parameters for the NREL 5MW and derating setting of 2.5 MW

P_{rated}	5 MW	ω_{rated}	12.1 rpm	v_{rated}	11.4 ms^{-1}
v_{ω}	10.6 ms^{-1}	P_{derated}	2.5 MW	ω_{derated}	10.21 rpm
v_{derated}	8.88 ms^{-1}	η	0.944		

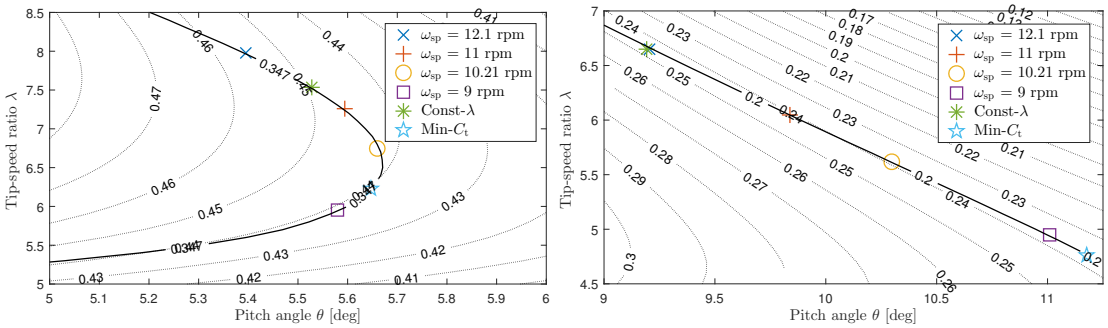

(a) The power demand is 2.5 MW with the wind speed of $v = 10\text{ms}^{-1}$. The power coefficient is $C_{\text{p}} = 0.348$.

(b) The power demand is 2.5 MW with the wind speed of $v = 12\text{ms}^{-1}$. The power coefficient is $C_{\text{p}} = 0.20$.

Figure 3: Operating points of different derating strategies on the power coefficient (solid black line) and thrust coefficient (dotted black line) contours for NREL 5MW turbine.

3.2. Analysis of the rotor speed set-point and derating strategies

Wind turbines are often operated in derated operations for numerous reasons, for example, to comply with the grid operators or optimise the wind farm efficiency. As discussed in Section 3.1, for a given power demand, the rotor speed set-point can be selected arbitrarily. To illustrate how the rotor speed set-point affect the turbine operating points, a baseline turbine NREL 5MW is considered with parameters listed in Table 1 and the demanded power is set as 50% of its rated power. For a given wind speed $v = 10\text{ms}^{-1}$, the power coefficient values can be derived based on (2), where $C_{\text{p}} \approx 0.347$ and it is depicted as a contour in Figure 3a. In addition, contour curves with different thrust coefficients are also depicted in Figure 3a. Similar to the power coefficient $C_{\text{p}}(\lambda, \theta)$, the thrust coefficient $C_{\text{t}}(\lambda, \theta) : \mathbb{R} \times \mathbb{R} \to \mathbb{R}$ is also a non-linear function of the pitch angle $\theta(t)$ and tip-speed ratio $\lambda(t)$, defined as follows:

$$C_{\text{t}}(\lambda, \theta) = \frac{F_{\text{t}}(t)}{\frac{1}{2}\rho\pi r^2 v^2(t)}, \tag{9}$$

Proposition 3.1. *For a specific value of the power coefficient $C_{\text{p}} \neq C_{\text{p}_{\max}}$, there exists a range of the thrust coefficient C_{t} that the turbine can operate with.*

Thus, based on Proposition 3.1, for a given P_{sp}, one can choose a rotor speed set-point ω_{sp} based on their design preferences.

Remark 1. *The readers may wonder the alternative method to achieve the same C_{p} by choosing the steady-state torque and pitch input arbitrarily. The main reason why we proposed to change the rotor speed set-point instead is to remain the continuity in the control architecture during nominal* (5) *and derating* (8) *conditions, which could avoid any undesired behaviour during switching nominal and derating operations.*

In the following, we will discuss several popular derating strategies.

Definition 3.4 (Derating strategy with $\omega_{\text{sp}} = \omega_{\text{rated}}(12.1\text{rpm})$ (Max-Ω))**.** *In this strategy, the rotational speed $\omega_{\text{sp}} = \omega_{\text{rated}}$ is at rated value once the wind speed $v \geq v_{\text{derated}}$ is enough for the turbine to operate at the derated power P_{derated}.*

This is one of the most widely used methods to down-regulate the turbine (e.g. [8]) because high rotational speed can store more kinetic energy that could provide inertia response to the power grid. The strategy is also known as the *maximum rotor speed (Max-Ω)* method in [12,13].

Definition 3.5 (Derating strategy with $\omega_{\text{sp}} = \omega_{\text{derated}}(10.21\text{rpm})$ (Const-Ω))**.** *The rotor speed remains at constant, namely, at the derated value $\omega_{\text{sp}} = \omega_{\text{derated}}$, once the operating wind speed reaches the derated value $v \geq v_{\text{derated}}$. Thus, its tip-speed ratio is always lower than that of the former strategies during derating.*

This distinct class of derating methods is known as *constant rotor speed (Const-Ω)* strategy in [12,13]. Notice that this approach operates at a lower tip-speed ratio and based on Figure 3a, the thrust coefficient is typically lower than the former strategy. The wake effects downstream, for example, the wind velocity deficit and added turbulence intensity, are in a positive relationship to the thrust coefficient of the upstream turbine [19,20]. Thus, this derating approach is favourable for wind farm operations compared to the former strategy.

Definition 3.6 (Derating strategy with constant tip-speed ratio (Const-λ))**.** *Unlike the former two strategies, in this approach, the tip-speed ratio is kept constant after the wind speed is above the derated value and until the rotor speed reaches its rated value, namely, $v_{\text{derated}} \leq v \leq v_{\omega}$. That implies the rotor speed increase from ω_{derated} to ω_{rated} over $v_{\text{derated}} \leq v \leq v_{\omega}$. After that, the rotor speed remains at rated and the strategy becomes similar to the Max-Ω approach.*

This strategy is a combination of the Max-Ω and Const-Ω methods. In the low wind speed, for example $v = 10\text{ms}^{-1}$, the derated turbine operates with a lower thrust coefficient than the Max-Ω strategy as shown in Figure 3a, whilst in the higher wind speed $v = 12\text{ms}^{-1}$, the Const-λ becomes the Max-Ω, so that it could store more kinetic energy for the grid services than the Const-Ω approach.

Next, as mentioned, turbine operating with a low C_{t} could generate less wake effect downstream. Close inspection of Figure 3a and 3b reveals that the operating points of the above-mentioned strategies are still far from the minimum C_{t}. Thus, we further investigate the following derating strategy:

Definition 3.7 (Derating strategy with minimum thrust coefficient (Min-C_{t}))**.** *From the power and thrust coefficient curves (for example, Figure 3a), a set of rotor speed set-points is calculated based on the tip-speed ratio that gives the minimum C_{t}.*

The downstream wake effects from the derated turbine with this strategy are at the minimal theoretically. However, notice that from Figure 3a and 3b, its operating points are relatively much closer to the stall region than the former strategies. A small perturbation in the wind speed might drive the derated turbine into the stalled operations. In order to gain a fuller picture, the following strategies are also proposed for comparison:

Definition 3.8 (Derating strategy with $\omega_{\text{sp}} = 11\text{rpm}$)**.** *This strategy is similar to the Const-Ω except that the rotor speed becomes $\omega_{\text{sp}} = 11\text{rpm}$ when the wind speed is above the derated value $v \geq v_{\text{derated}}$.*

Definition 3.9 (Derating strategy with $\omega_{\text{sp}} = 9\text{rpm}$)**.** *Similarly, in this strategy, the rotor speed goes down to $\omega_{\text{sp}} = 9\text{rpm}$ once the wind speed reaches $v \geq v_{\text{derated}}$.*

In summary, the operating points of all derating strategies are illustrated in Figure 3a and 3b. One generalised rule can be seen is that the derated turbine with a lower rotor speed set-point ω_{sp} tends to operate with a lower thrust coefficient C_{t}. However, the analysis presented in this section only considered the steady-state operating points. Given wind turbines are constantly subjected to unsteady wind speed, thus, further investigations are conducted in the next section.

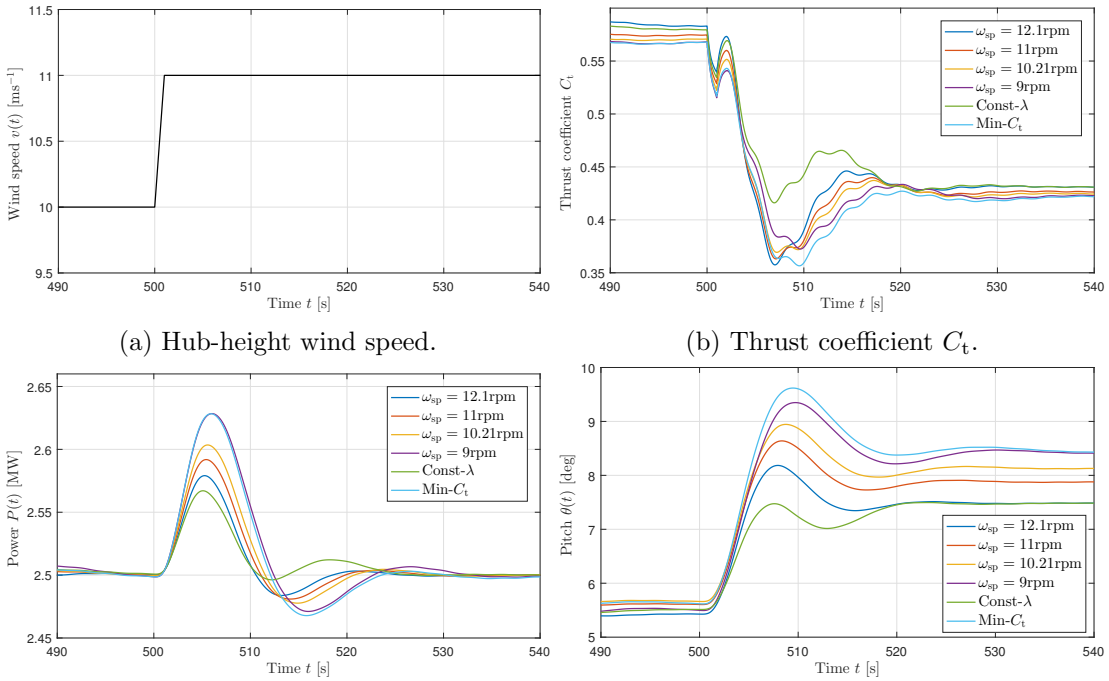

(a) Hub-height wind speed.

(b) Thrust coefficient C_t.

(c) Power output of the derated turbine.

(d) Pitch angle of blade 1.

Figure 4: Performance of derating strategy under step wind case.

4. Numerical simulations

4.1. Simulation environment and settings

The turbine model used in this study is the NREL 5MW reference turbine [17] based on the open-source FAST code [21]. This model includes many degrees-of-freedom such as the tower fore-after, side-to-side, in addition to the rotor and blade dynamics. Three wind fields were considered in this study: one with step changes in the wind speed and another two with time-varying turbulent wind fields generated by the TurbSim code [22]. Comparisons were conducted with all derating strategies discussed in Section 3.2.

4.2. Step wind case

In these closed-loop simulations, all derating control strategies were demanded to operate at 50% of the rated power, which is $P_{\text{sp}} = 2.5$MW. A full step wind case was chosen, where an increase in the hub-height wind speed from 3 ms^{-1} up to 25 ms^{-1} with an increment of 1 ms^{-1} every 50 seconds. Figure 4a shows a time-history of the wind step from 10ms^{-1} to 11ms^{-1}. Figure 4b demonstrates the thrust coefficient of the derated turbine with different derating strategies. It is clearly shown that the turbines with a lower rotor speed set-point ω_{sp} resulted in a lower thrust coefficient C_{t}, and particularly, the lowest C_{t} was achieved by the Min-C_{t} approach. In addition, the turbine with the Const-λ strategy operated at a lower C_{t} compared to that with the Max-Ω method before 500s. After the wind speed reached 11ms^{-1}, the difference became less significant as the Const-λ strategy becomes the Max-Ω method in higher wind speed operations.

Figure 4c shows the performance of the power regulation of different derating strategies. As the rotor speed set-point ω_{sp} was lower, the transient behaviour on the power output became worse. This also applied to the blade pitch activities in Figure 4d. One outstanding derating method is the Const-λ approach with minimum variations in the power output and pitch activity.

The performance of the turbine structural fatigue damage is summarised in Table 2. The repetitive loads were quantified as the fatigue damage equivalent loads (DEL), characterised by

Table 2: Performance of derating strategies under a step wind case.

ω_{sp} [rpm]	12.1	11	10.4	9	Const-λ	Min-C_{t}
DEL(M_{t})	100.00	86.37	83.53	81.12	86.45	80.23
DEL(τ_{dt})	100.00	100.95	101.87	104.23	102.10	106.23
Pitch travel θ_{sum}	100.00	100.77	113.97	124.99	94.09	130.14

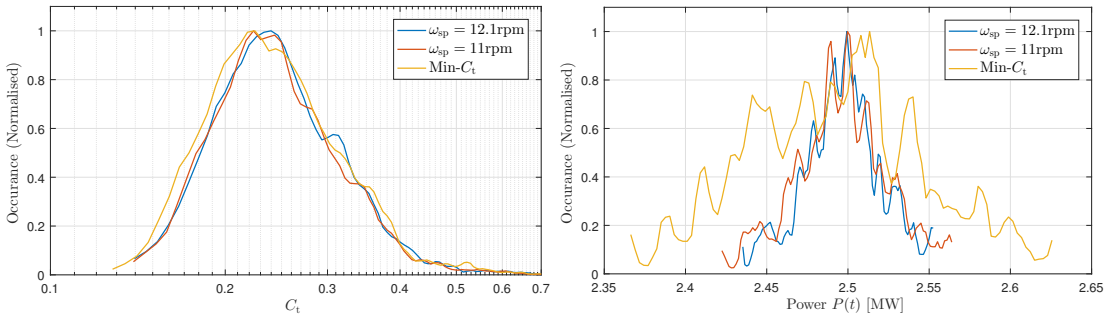

(a) Histogram of the thrust coefficient.

(b) Histogram of the power output.

Figure 5: Performance of derating strategies under turbulent wind field of the mean speed 12 ms^{-1} and turbulence intensity 14% .

the rain-flow counting method [23]. In Table 2, the effect of derating strategies on the DEL of the fore-aft tower base bending moment (M_{t}) is consistent with the effect on thrust coefficient. As the rotor speed set-point is lower, the DEL of the tower structure decreases. Nonetheless, for the DEL of the drive-train torque (τ_{dt}), a lower rotor speed set-point tends to result in a higher value. This is expected as the power is the product of the rotor speed and torque. To sum up, among the derating strategies, the Const-λ strategy was quite outstanding for all aspect, whilst the Min-C_{t} could achieve the lowest thrust coefficient.

4.3. Time-varying turbulent wind speed

So far, the performance was evaluated with the wind speed that was rather steady. As the perturbation in the wind speed was larger, it could drive the turbine into the stalled operations if derating operating points were too close to the stalled region. Thus, to evaluate the robustness of the strategies, the closed-loop simulations in this section were performed under turbulent wind fields characterised by the mean speed of 12 ms^{-1} and 14 ms^{-1} with turbulence intensity of 14%.

Figure 5a illustrates the histogram of the thrust coefficient C_{t} of the selected derating strategies. Comparing derating strategies with ω_{sp} = 12.1rpm and 11rpm, the derated turbine with a lower rotor speed set-point (e.g. strategies with ω_{sp} = 11rpm and Min-C_{t}) operated with a distribution of slightly lower thrust coefficient C_{t}, which is consistent to the performance in the step wind case. However, their power variations were the worse than the nominal case as revealed in Figure 5b, especially the Min-C_{t} approach. Further measures of the fatigue damage are summarised in Table 3. It can be seen that the DEL of the tower structure by the Min-C_{t} strategy was significantly higher than the other derating methods. This is the consequence of operating at the stalled region occasionally. Moreover, as for the rest of derating strategies, when the rotor speed set-point is lower, the DEL of the tower also tends to be lower.

Moreover, the results obtained from simulations with higher wind speed v = 14ms^{-1} was summarised in Table 4. Notice that the tower fatigue damage was higher for derating strategies with ω_{sp} = 9rpm than 10.4rpm. This is because the derating strategies with a lower rotor speed reference began to operate at the stall region. Another observation is that the Const-λ

Table 3: Performance of derating strategies under turbulent wind field of the mean speed 12ms^{-1} and turbulent intensity 14%.

ω_{sp} [rpm]	12.1	11	10.4	9	Const-λ	Min-C_{t}
DEL(M_{t})	100.00	93.62	91.83	86.25	92.34	168.29
DEL(τ_{dt})	100.00	111.24	102.86	94.06	110.34	86.02
Pitch travel θ_{sum}	100.00	105.16	112.05	123.65	98.23	148.32

Table 4: Performance of derating strategies under turbulent wind field of the mean speed 14ms^{-1} and turbulent intensity 14%.

ω_{sp} [rpm]	12.1	11	10.4	9	Const-λ	Min-C_{t}
DEL(M_{t})	100.00	91.20	82.23	96.28	100.00	120.74
DEL(τ_{dt})	100.00	112.17	108.61	91.70	100.00	83.82
Pitch travel θ_{sum}	100.00	90.52	103.54	100.30	100.00	127.69

performed identically as the Max-Ω as expected.

In summary, the derated turbine with a lower rotor speed set-point tends to result in a lower tower fatigue damage, higher drive-train loads and also an increase in blade pitch activities. Nonetheless, when derating the rotor speed, one needs to ensure the turbine is operating away from the stalled region. From some preliminary results, it can be concluded that it is safe to design derating strategies with the rotor speed set-point between the rated value ω_{rated} and derated value ω_{derated} (i.e. 10.4 rpm in this case). Also, the trade-off between tower fatigue and drive-train loads and pitch activities needs to be taken in account.

5. Conclusion

In this paper, the studies of the derating strategies with different rotor speed set-point were presented, showing that the rotor speed set-point is in positive relationship to the thrust coefficient. In addition, the derated turbine operating at a lower rotor speed resulted in a lower tower structure fatigue damage, but a higher drive-train loading and blade pitch activities. This work also showed that a low rotor speed set-point without care could lead the turbine to the stalled operations, where the fatigue damage on the tower would increase significantly. In the future work, we investigate the thrust coefficient on the wake effect and also model predictive control (e.g [24, 25]) to ensure the derating strategies operating away from the stalled region.

Acknowledgement

This research was supported by the PowerKey project (EUDP Project No. 12558).

References

[1] Jacob Aho, Andrew Buckspan, Lucy Pao, and Paul Fleming. An Active Power Control System for Wind Turbines Capable of Primary and Secondary Frequency Control for Supporting Grid Reliability. *AIAA/ASME Wind Symposium*, pages 1–13, 2013.

[2] S Boersma, B.M. Doekemeijer, P.M.O. Gebraad, P.A. Fleming, J Annoni, A.K. Scholbrock, J.A. Frederik, and J-W. van Wingerden. A tutorial on control-oriented modeling and control of wind farms. In *2017 American Control Conference (ACC)*, pages 1–18. IEEE, may 2017.

[3] Jacob Aho, Andrew Buckspan, and Jason H. Laks. A tutorial of wind turbine control for supporting grid frequency through active power control. *Proc. of the American Control Conference*, pages 3120–3131, 2012.

[4] H. Aa. Madsen, G. C. Larsen, T. J. Larsen, N. Troldborg, and R. Mikkelsen. Calibration and Validation of the Dynamic Wake Meandering Model for Implementation in an Aeroelastic Code. *Journal of Solar Energy Engineering*, 132(4):041014, 2010.

[5] Torben J. Larsen, Helge Aa. Madsen, Gunner C. Larsen, and Kurt S. Hansen. Validation of the dynamic wake meander model for loads and power production in the Egmond aan Zee wind farm. *Wind Energy*, 16(4):605–624, may 2013.
[6] LY Pao and KE Johnson. A tutorial on the dynamics and control of wind turbines and wind farms. *Proc. of ACC*, 2009.
[7] W.H. Lio, J.A. Rossiter, and B.L. Jones. A review on applications of model predictive control to wind turbines. In *2014 UKACC International Conference on Control, CONTROL 2014 - Proceedings*, 2014.
[8] V Spudić, M Jelavić, M Baotić, M Vašak, and P Nedjeljko. Deliverable 3.3 - Distributed Control of Large-Scale Offshore Wind Farms. *Ict-Aeolus.Eu*, 2008.
[9] Benjamin Biegel, Daria Madjidian, Vedrana Spudić, Anders Rantzer, and Jakob Stoustrup. Distributed low-complexity controller for wind power plant in derated operation. *Proceedings of the IEEE International Conference on Control Applications*, pages 146–151, 2013.
[10] Ameet S. Deshpande and Rhonda R. Peters. Wind turbine controller design considerations for improved wind farm level curtailment tracking. *IEEE Power and Energy Society General Meeting*, pages 1–6, 2012.
[11] Zhichao Zhou and Chengshan Wang. Output power curtailment control of variable-speed variable-pitch wind turbine generators. *Asia-Pacific Power and Energy Engineering Conference, APPEEC*, 2015-March(March), 2014.
[12] Mahmood Mirzaei, Mohsen Soltani, Niels K. Poulsen, and Hans H. Niemann. Model based active power control of a wind turbine. *2014 American Control Conference*, (July 2016):5037–5042, 2014.
[13] Mahmood Mirzaei, Tuhfe Gocmen, Gregor Giebel, Poul Ejnar Sorensen, and Niels K Poulsen. Turbine Control strategies for wind farm power optimization. In *2015 American Control Conference (ACC)*, pages 1709–1714. IEEE, jul 2015.
[14] Christos Galinos, Torben J Larsen, and Mahmood Mirzaei. Impact on wind turbine loads from different down regulation control strategies. In *DeepWind2018*, 2018.
[15] Kuichao Ma, Jiangsheng Zhu, Mohsen Soltani, Amin Hajizadeh, and Zhe Chen. Wind turbine down-regulation strategy for minimum wake deficit. *2017 11th Asian Control Conference (ASCC)*, pages 2652–2656, 2017.
[16] Jiangsheng Zhu, Kuichao Ma, Mohsen Soltani, Amin Hajizadeh, and Zhe Chen. Comparison of loads for wind turbine down-regulation strategies. *2017 11th Asian Control Conference (ASCC)*, pages 2784–2789, 2017.
[17] J. Jonkman, S. Butterfield, W. Musial, and G. Scott. Definition of a 5-MW Reference Wind Turbine for Offshore System Development. Technical report, National Renewable Energy Laboratory (NREL), Golden, CO, feb 2009.
[18] Morten Hartvig Hansen ; Lars Christian Henriksen. *Basic DTU Wind Energy controller*. Number January. 2013.
[19] N O Jensen. A note on wind generator interaction. Technical report, Risø National Laboratory, Roskilde, Denmark, 1983.
[20] T N Jensen, T Knudsen, and T Bak. Fatigue minimising power reference control of a de-rated wind farm. In *Journal of Physics: Conference Series*, volume 753, page 052022, 2016.
[21] J. M. Jonkman and M.L. Buhl Jr. FAST User's Guide. Technical report, National Renewable Energy Laboratory (NREL), 2005.
[22] B.J. Jonkman. TurbSim User's Guide. Technical report, National Renewable Energy Laboratory (NREL), 2009.
[23] Herbert J Sutherland. On the Fatigue Analysis of Wind Turbines. Technical report, Sandia National Laboratories (SNL), Albuquerque, NM, and Livermore, CA, jun 1999.
[24] W. H. Lio, J. A. Rossiter, and B. Ll. Jones. Predictive control design on an embedded robust output-feedback compensator for wind turbine blade-pitch preview control. In *2016 European Control Conference*, 2016.
[25] W H Lio, B Ll. Jones, and J A Rossiter. Preview predictive control layer design based upon known wind turbine blade-pitch controllers. *Wind Energy*, 20(7):1207–1226, 2017.